A novel electrochemical aptasensor for fumonisin B1 determination using DNA and exonuclease-I as signal amplification strategy

Min Wei (wei_min80@163.com)
Henan University of Technology
Fei Zhao
Henan University of Technology
Shuo Feng
Henan University of Technology
Huali Jin
Henan University of Technology

Research article

Keywords: Electrochemical aptasensor: Fumonisin B1: Exonuclease-I: G-rich DNA: Methylene blue

Posted Date: October 30th, 2019

DOI: https://doi.org/10.21203/rs.2.12922/v4

Version of Record: A version of this preprint was published on November 9th, 2019. See the published version at https://doi.org/10.1186/s13065-019-0646-z.

Abstract

In this work, using DNA and exonuclease-I (Exo-I) as signal amplification strategy, a novel and facile electrochemical aptasensor was constructed for fumonisin B1 (FB1) detection. The G-rich complementary DNA (cDNA) was immobilized onto the electrode surface. Then, aptamer of FB1 was hybridized with cDNA to form double-stranded DNA. In the absence of FB1, double-stranded DNA and G-rich cDNA on the electrode surface promoted effectively methylene blue (MB) enrichment and amplified the initial electrochemical response. In the presence of FB1, the combination of aptamer and FB1 led to the release of aptamer from the electrode surface and the expose of 3' end of single-stranded cDNA. When Exo-I was added onto the electrode surface, the single-stranded cDNA was degraded in the 3'-5' direction. The decrease of double-stranded DNA and G-rich cDNA resulted in the less access of MB to the electrode surface, which decreased the electrochemical signal. The experimental conditions including incubation time of FB1, the amount of Exo-I and incubation time of Exo-I were optimized. Under the optimal conditions, the linear relationship between the change of peak current and the logarithmic concentration of FB1 was observed in the range of 1.0×10-3-1000ng·mL−1 with a low limit of detection of 0.15 pg·mL−1. The experimental results showed that the prepared aptasensor had acceptable specificity, reproducibility, repeatability and stability. Therefore, this proposed aptasensor has a potential application in the food safety detection.

Introduction

As the metabolic product of Fusarium moniliforme Sheld, fumonisin B_1 (FB_1) is a kind of the most toxic and prevalent fumonisins [1]. FB_1 can contaminate various food and feedstuff such as corn, wheat, rice, peanut, beer, and animal feed. A large number of studies have reported that FB_1 can cause serious diseases such as horse white matter softening, nephrotoxicity, hepatotoxicity and liver cancer [2,3]. Therefore, it is necessary to monitor FB_1 for food safety and human health.

Among the various methods for FB_1 detection [4-7], the electrochemical aptasensor has attracted widespread attention due to their low cost, simple operation, high selectivity and affinity, chemical stability, and easy storage [8,9]. Recently, with the advantages including effective amplification strategy, easy design, simple operation and rapid reaction, the nuclease-based electrochemical aptasensor has become research focus [10,11]. Among the different nucleases, exonuclease I (Exo-I) has attracted increasing attention, owing to its structure-sensitive digestion for the single-stranded DNA in the direction of 3' to 5', low cost, good specificity and buffer compatibility [12-14]. As a kind of electrochemical signal probe, methylene blue (MB) can highly interact with G-rich single-stranded DNA and double-stranded DNA, and is therefore suitable for the application in electrochemical aptasensor [15,16].

Herein, based on MB, Exo-I, aptamer of FB_1 (Apt) and G-rich cDNA, a novel signal-off sensor was firstly designed for the electrochemical detection of FB_1. The existing double-stranded DNA on the electrode surface, came from the hybridization of Apt and G-rich cDNA, enriched abundant MB and amplified the initial electrochemical response. In the presence of FB_1, the formation of Apt-FB_1 made aptamer release from the electrode surface. Then, the effect of Exo-I on G-rich cDNA of the electrode surface resulted in the less access

of MB, which further decreased the electrochemical signal and amplified ΔI. The change of MB electrochemical signal can be applied for FB_1 detection.

In virtue of the favorable combination of MB with double-stranded DNA and G-rich cDNA, and the advantages of Exo-I including easy design, simple operation, high amplification efficiency and excellent selectivity, the proposed signal amplification strategies can save the tedious preparation process and is beneficial to the experimental stability.

Experimental

Materials and chemicals

The used oligonucleotides were provided by Sangon Biological Engineering Technology & Services Co. Ltd. (Shanghai, China), and their sequences were as follows: cDNA: 5'-SH-GAG GGG TGG GCG GGA GGG AGA TTG CAC GGA CTA TCT AAT TGA ATA AGC-3'. Apt: 5'-ATA CCA GCT TAT TCA ATT AAT CGC ATT ACC TTA TAC CAG CTT ATT CAA TTA CGT CTG CAC ATA CCA GCT TAT TCA AGT AGA TAG TAA GTG CAA TCT-3'. FB_1 and Exo-I were purchased from Acros and TaKaRa, respectively. 0.05 M of pH 7.4 Tris-HCl buffer (containing 0.05 M Tris, 0.2 M NaCl and 0.001 M EDTA) was used.

Apparatus

The CHI 660E Electrochemical Workstation was used for the electrochemical experiments (Shanghai Chenhua Instrument Corporation, China). The gold electrode (AuE) was used as working electrode. Differential pulse voltammetry (DPV) and electrochemical impedance spectroscopy (EIS) were used for the electrochemical measure.

Fabrication and mechanism of the aptasensor

The fabrication and mechanism of the aptasensor were shown in Fig.1. 5 μL of 1 μM SH-cDNA was dropped on the AuE surface for immobilization at 37°C. Then, the AuE was washed by Tris-HCl buffer to remove the unbound cDNA. After that, 5 μL of 6-mercapto-1-hexanol (MCH) was dropped to block the untreated sites. Next, 5 μL of 1 μM Apt was hybridized with cDNA for 2 h at 37°C to obtain the aptasensor Apt/cDNA/AuE.

When FB_1 was absent, cDNA and Apt could not be degraded by Exo-I because that the 3’ end of both cDNA and Apt were protected by the formation of double-stranded DNA. MB could intercalate into G-rich cDNA and double-stranded DNA, and produce a strong current signal. When FB_1 was present, the complex of Apt and FB_1 was formed and released from the surface of the electrode, leading to the expose of 3' end of single-stranded cDNA on the electrode surface. When Exo-I was added onto the electrode surface, the single-stranded cDNA was degraded in the 3’-5’ direction. The decrease of double-stranded DNA and G-rich cDNA resulted in the less access of MB to the electrode surface and the decrease of the electrochemical signal. The change of MB electrochemical signal can be applied for FB_1 detection.

Results And Discussion

Electrochemical characterization of the prepared aptasensor

Fig.2 showed the EIS characterization for the aptasensor fabrication. The charge transfer resistance (R_{ct}) increased from 251.3 ohm of the bare AuE (a) to 1219 ohm of the cDNA/AuE (b), indicating that the cDNA was immobilized to the electrode surface. For the Apt/cDNA/AuE (c), the R_{ct} was increased to 1381 ohm, indicating that Apt hybridized successfully with cDNA on the electrode surface. After the Apt/cDNA/AuE was incubated by 1 μg·mL^{-1} FB_1 and Exo-I respectively, the R_{ct} (d) was decreased to 836 ohm. This was because that Apt was specifically combined with FB_1 and released from the electrode, and cDNA was digested by Exo-I due to the expose of its 3' end, resulting in the less negative charge on the electrode surface.

The detection of FB_1 on Apt/cDNA/AuE sensor

Fig.3 showed the DPV results of MB on the Exo-I/Apt/cDNA/AuE (a), FB_1/Apt/cDNA/AuE (b) and Exo-I/FB_1/Apt/cDNA/AuE (c) in Tris-HCl buffer. In the absence of FB_1, the Exo-I/Apt/cDNA/AuE showed an initial peak current of 7.29 μA (a). With the addition of 1 μg·mL^{-1} FB_1, the peak current of FB_1/Apt/cDNA/AuE (b) decreased to 4.02 μA. This is because that in the presence of FB_1, the formation of Apt-FB_1 composite made Apt release from double-stranded DNA on the electrode surface, resulting in that the amounts of MB intercalated into the double-stranded DNA were decreased. After the addition of Exo-I, the DPV value of Exo-I/FB_1/Apt/cDNA/AuE (c) further decreased to 2.41 μA, indicating that Exo-I could digest the single-stranded cDNA on the electrode surface and achieve the signal amplification.

Optimization of the aptasensor

Fig.4 showed the effect of FB_1 incubation time (A), Exo-I amount (B) and Exo-I incubation time (C) on the electrochemical signal. As shown in Fig.4 A, it can be seen that ΔI increased with the increasing of FB_1 incubation time and reached the maximum of 5.3 μA at 10 min. Therefore, 10 min was selected as the optimal FB_1 incubation time. As can be seen from Fig.4 B, ΔI increased with increasing of Exo-I amount and reached the maximum at 5 U, then decreased when the amount was further increased. This may due to that the limit of active surface area on the fabricated electrode led to the inefficiency of redundant Exo-I. So, 5 U of Exo-I was used for the subsequent experiments. As shown in Fig.4 C, the ΔI increased quickly with increasing the incubation time in the first 30 min, then changed slightly when the incubation time was more than 30 min. Therefore, 30 min was used as the optimal Exo-I incubation time.

Analytical performance of the designed aptasensor

Fig.5 showed the calibration plot of the fabricated aptasensor for FB_1 detection. With the concentration range of 1×10^{-3}~1000 ng·mL^{-1}, a linear relationship between ΔI and Lg [C_{FB1}] was observed, and the linear regression equation was $\Delta I=0.71036\ Lg[C_{FB1}]+3.18714$ ($R^2=0.998$). The limit of detection (LOD) was calculated to be 0.15 pg·mL^{-1} at a signal-to-ratio of 3. Compared to the previous reports, the designed aptasensor obtained a wider linear range and lower LOD, and the result was shown in Table 1.

Specificity, reproducibility, repeatability and stability

The specificity of the aptasensor to ochratoxin A (OTA), zearalenone (ZEA) and aflatoxin B_1 (AFB_1) was studied, and the results were shown in Fig.6. Only when the prepared aptasensor was incubated in FB_1, the peak current decreased significantly, indicating that the designed aptasensor had good specificity and could meet the experimental requirements.

Under the optimized conditions, the reproducibility and the repeatability of the fabricated aptasensor was respectively evaluated with inter-assay and intra-assay. Under the same experimental conditions, five fabricated aptasensors were tested by monitoring the peak current of MB with 1 $\mu g \cdot mL^{-1}$ FB_1 on the FB_1/Apt/cDNA/AuE, and a relative standard deviation (RSD) of 5.72% was calculated, implying that the fabricated sensor had satisfactory reproducibility. The one aptasensor was investigated by monitoring the peak current of MB in the presence of 1 $\mu g \cdot mL^{-1}$ FB_1 for five replicate determinations under the same conditions, and RSD of 5.38% was calculated, implying that the fabricated aptasensor had acceptable repeatability.

For the study on stability of the fabricated aptasensor, the peak current of MB on the three Exo-I/Apt/cDNA/AuE was detected, and the average peak current is 7.21 μA. Then the fabricated aptasensors were stored at 4℃. After a 35-day storage period, the average peak current of MB on the Exo-I/Apt/cDNA/AuE was 6.14 μA, and the aptasensor retained 85.2% of its initial current response, indicating the acceptable stability.

Analysis of FB_1 in food samples

The accuracy of the fabricated aptasensor was evaluated by studying the recovery of FB_1 in beer samples and corn samples, and the results were shown in Table 2. Beer samples were filtrated through a 0.45 μm membrane, and used for subsequent tests by spiking different concentrations of FB_1. Non-contaminated corn samples were finely milled to obtain corn powder, and 0.5 g of the corn powder was extracted with methanol-water (60:40, v/v. 5 mL) using an orbital shaker for 30 min. After centrifugation for 15 min, the extract was used for analysis by spiking different concentrations of FB_1. By addition of 100 $ng \cdot mL^{-1}$, 1 $ng \cdot mL^{-1}$ and 1×10^{-2} $ng \cdot mL^{-1}$ of FB_1, for the beer samples, the average recoveries were 88.5%, 96.1% and 98.6% respectively. For the corn samples, the average recoveries were 91.4%, 87.3% and 106.8% respectively. These results indicated that the fabricated aptasensor can be applied in FB_1 detection of the food samples.

Conclusion

In summary, on the basis of DNA and Exo-I as signal amplification strategy, a novel and facile signal-off aptasensor was developed for FB_1 detection. Utilizing the favorable combination of MB with double-stranded DNA and G-rich cDNA, the specific DNA was designed to enrich abundant MB for initial signal amplification. On the other hand, with the advantages of easy design, simple operation, high amplification efficiency and excellent selectivity, Exo-I was used to design a novel signal-off aptasensor for amplifying the ΔI. These two signal amplification strategies can avoid the complicated nanomaterial preparation and instability. As a

result, this proposed aptasensor showed the favorable performance with simple preparation, good selectivity, reproducibility, repeatability, stability as well as a wider linear range with lower LOD, providing a promising potential for application in food safety detection.

List Of Abbreviations

DNA: deoxyribonucleic acid

Exo-I: exonuclease-I

FB_1: fumonisin B_1

cDNA: complementary DNA

MB: methylene blue

Apt: aptamer of FB_1

DPV: differential pulse voltammetry

EIS: electrochemical impedance spectroscopy

MCH: 6-mercapto-1-hexanol

AuE: the gold electrode

R_{ct}: the charge transfer resistance

ΔI: the difference of peak current

LOD: limit of detection

OTA: ochratoxin A

ZEA: zearalenone

AFB_1: aflatoxin B_1

RSD: relative standard deviation

Declarations

Availability of data and materials

All data generated or analyzed during this study are included in this published article. We have presented all data in the form of tables and figures.

Competing interests

The authors declare that they have no competing interests.

Funding

This study was supported by the Natural Science Foundation of Henan Province (182300410188) in the design of the study, and collection, analysis, and interpretation of data; supported by the Fundamental Research Funds for the Henan Provincial Colleges and Universities in Henan University of Technology (2016RCJH04) in collection, analysis, and interpretation of data; supported by Key Scientific and Technological Project of Henan Province (192102310255) in writing the manuscript.

Acknowledgements

Not applicable.

Authors' contributions

MW, FZ, SF and HJ conceived and designed the experiments; FZ and SF performed the experiments; MW and HJ analyzed the data; MW, FZ, and SF wrote and modified the paper. All authors read and approved the final manuscript.

References

1. Chen XW, Liang Y, Zhang WJ, Leng YK, Xiong YH (2018) A colorimetric immunoassay based on glucose oxidase-induced AuNP aggregation for the detection of fumonisin B_1. Talanta 186: 29-35
2. Chen C, Mitchell NJ, Gratz J, Houpt ER, Gong YY, Egner PA, Groopman JD, Riley RT, Showker JL, Svensen E, Mduma ER, Patil CL, Wu F (2018) Exposure to aflatoxin and fumonisin in children at risk for growth impairment in rural tanzania. Environ Int 115: 29-37
3. Munawar H, Smolinska-Kempisty K, Cruz AG, Canfarotta F, Piletska E, Karim K, Piletsky SA (2018) Molecularly imprinte polymer nanoparticle-based assay (MINA): application for fumonisin B_1 determination. Analyst 143: 3481-3488
4. Andrade GCRM, Pimpinato RF, Francisco JG, Monteiro SH, Calori-Domingues MA, Tornisielo VL (2018) Evaluation of mycotoxins and their estimated daily intake in popcorn and cornflakes using LC-MS techniques. LWT-Food Sci Technol 95: 240-246.
5. Liu R, Li W, Cai TT, Deng Y, Ding Z, Liu Y, Zhu XR, Wang X, Liu J, Liang BW, Zheng TS, Li JL (2018) TiO_2 Nanolayer-Enhanced fluorescence for simultaneous multiplex mycotoxin detection by aptamer microarrays on a porous silicon surface. ACS Appl Mater Inter 10: 14447-14453
6. Ren CC, Li HM, Lu XT, Qian J, Zhu MY, Chen W, Liu Q, Hao N, Li HN, Wang K (2017) A disposable aptasensing device for label-free detection of fumonisin B_1 by integrating PDMS film-based micro-cell and screen-printed carbon electrode. Sens Actuators B 251: 192-199
7. Zhang W, Xiong H, Chen MM, Zhang XH, Wang SF (2017) Surface-enhanced molecularly imprinted electrochemiluminescence sensor based on Ru@SiO_2 for ultrasensitive detection of fumonisin B_1. Biosens Bioelectron 96: 55-61

8. Chen XJ, Huang YK, Duan N, Wu SJ, Xia Y, Ma XY, Zhu CQ, Jiang Y, Ding Z, Wang ZS (2014) Selection and characterization of single stranded DNA aptamers recognizing fumonisin B_1. Microchim Acta 181: 1317-1324
9. Wang CQ, Qian J, An KQ, Huang XY, Zhao LF, Liu Q, Hao N, Wang K (2017) Magneto-controlled aptasensor for simultaneous electrochemical detection of dual mycotoxins in maize using metal sulfide quantum dots coated silica as labels. Biosens Bioelectron 89: 802-809
10. Luan Q, Miao YB, Gan N, Cao YT, Li TH, Chen YJ (2017) A POCT colorimetric aptasensor for streptomycin detection using porous silica beads-enzyme linked polymer aptamer probes and exonuclease-assisted target recycling for signal amplification. Sens Actuators B 251: 349-358
11. Yan MM, Bai WH, Zhu C, Huang YF, Yan J, Chen AL (2016) Design of nuclease-based target recycling signal amplification in aptasensors. Biosens Bioelectron 77: 613-623
12. Abnous K, Danesh NM, Alibolandi M, Ramezani M, Emrani AS, Zolfaghari R, Taghdisi SM (2017) A new amplified π-shape electrochemical aptasensor for ultrasensitive detection of aflatoxin B_1. Biosens Bioelectron 94: 374-379
13. Taghdisi SM, Danesh NM, Ramezani M, Abnous K (2017) Electrochemical aptamer based assay for the neonicotinoid insecticide acetamiprid based on the use of an unmodified gold electrode. Microchim Acta 184: 499-505
14. Xing XJ, Xiao WL, Liu XG, Zhou Y, Pang DW, Tang HW (2016) A fluorescent aptasensor using double-stranded DNA/graphene oxide as the indicator probe. Biosens Bioelectron 78: 431
15. Wei M, Feng S (2017) A signal-off aptasensor for the determination of Ochratoxin A by differential pulse voltammetry at a modified Au electrode using methylene blue as an electrochemical probe. Anal Methods 9: 5449-5454
16. Wei M, Zhang W (2017) A novel impedimetric aptasensor based on AuNPs-carboxylic porous carbon for the ultrasensitive detection of ochratoxin A. RSC Adv 7: 28655-28660
17. Quan Y, Zhang Y, Wang S, Lee NJ, Kennedy IR (2006) A rapid and sensitive chemiluminescence enzyme-linked immunosorbent assay for the determination of fumonisin B_1 in food samples. Anal Chim Acta 580: 1-8
18. Mirasoli M, Buragina A, Dolci LS, Simoni P, Anfossi L, Giraudi G, Roda A (2012) Chemiluminescence-based biosensor for fumonisins quantitative detection in maize samples. Biosens Bioelectron 32: 283-287
19. Wu SJ, Duan N, Li XL, Tan GL, Ma XY, Xia Y, Wang ZP, Wang HX (2013) Homogenous detection of fumonisin B_1 with a molecular beacon based on fluorescence resonance energy transfer between $NaYF_4$:Yb, Ho upconversion nanoparticles and gold nanoparticles. Talanta 116: 611-618
20. Yang XX, Zhou XP, Zhang X, Qing Y, Luo M, Liu X, Li CR, Li YL, Xia HM, Qiu JF (2015) A highly sensitive electrochemical immunosensor for Fumonisin B_1 detection in corn using single-walled carbon nanotubes/chitosan. Electroanalysis 27: 2679-2687
21. Lu L, Seenivasan R, Wang YC, Yu JH, Gunasekaran S (2016) An electrochemical immunosensor for rapid and sensitive detection of mycotoxins Fumonisin B_1 and deoxynivalenol. Electrochim Acta 213: 89-97

22. Jodra A, Angel Lopez M, Escarpa A (2015) Disposable and reliable electrochemical magneto immunosensor for Fumonisins simplified determination in maize-based foodstuffs. Biosens Bioelectron 64: 633-638
23. Shi ZY, Zheng YT, Zhang HB, He CH, Wu WD, Zhang HB (2015) DNA electrochemical aptasensor for detecting Fumonisins B_1 based on graphene and thionine nanocomposite. Electroanalysis 27: 1097-1103

Tables

Table 1 Comparison with other reported methods for FB_1 detection

Method	Amplification strategy	Linearity ($ng \cdot mL^{-1}$)	LOD ($ng \cdot mL^{-1}$)	Ref.
Chemiluminescence &enzyme-linked immunosorbent	ECL-ELISA based on anti-FB_1 IgG and HRP	0.14~0.9	0.09	[17]
Chemiluminescence	Charge-coupled device	2.5~500	2.5	[18]
Fluorescence	Anti apt/Apt-NH_2/TiO_2-PSi	0.001~10	0.21×10^{-3}	[5]
Fluorescence resonance energy transfer	AuNPs-MB-UCNPs	0.01~100	0.01	[19]
Electrochemiluminescence	MIP/Ru@SiO_2/CS/AuNPs/GCE	1×10^{-3}~100	0.35×10^{-3}	[6]
Electrochemical immunosensor	AP-anti-antibody/anti-FB_1/FB_1-BSA-SWNTs/CS/GCE	0.01~1000	2×10^{-3}	[20]
Electrochemical immunosensor	Ab-AuNPs-PPy/ErGO-SPE	200~4500	4.2	[21]
Electrochemical magneto immunosensor	FB1-HRP/Ab-FB_1/MB&protein G/CSPE	0.73~11.2	0.33	[22]
Electrochemical aptasensor	Apt-AuNPs-SPCE	1×10^{-2}~50	3.4×10^{-3}	[7]
Electrochemical aptasensor	GS-TH/S2/S1/Au/GCE	1×10^{-3}~1000	1×10^{-3}	[23]
Electrochemical aptasensor	Exo-I/Apt/cDNA/AuE	1×10^{-3}~1000	0.15×10^{-3}	This work

Table 2 Recovery of FB_1 in food samples

Sample	Added ($ng \cdot mL^{-1}$)	Average Found ($ng \cdot mL^{-1}$)	Average Recovery (%)	RSD (%) n=3
Beer	100	88.5	88.5	1.75
	1	0.961	96.1	2.25
	1×10^{-2}	0.986×10^{-2}	98.6	5.65
Corn	100	91.4	91.4	4.76
	1	0.873	87.3	7.79
	1×10^{-2}	1.068×10^{-2}	106.8	6.34

Figures

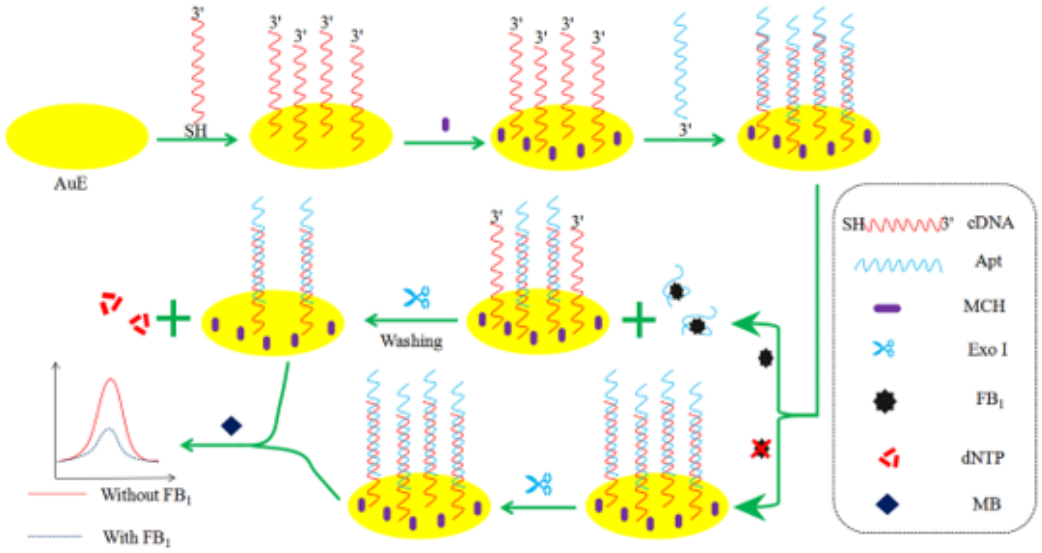

Figure 1

The fabrication and mechanism of the aptasensor

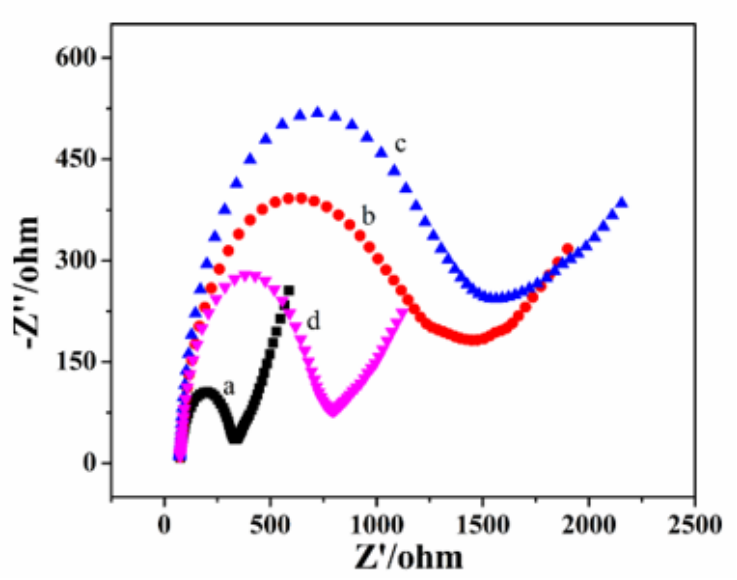

Figure 2

EIS of 10 mM [Fe(CN)6]3-/4- containing 0.1 M KCl on the AuE (a), the cDNA/AuE (b), and the Apt/cDNA/AuE before (c) and after (d) addition of FB1 and Exo-I.

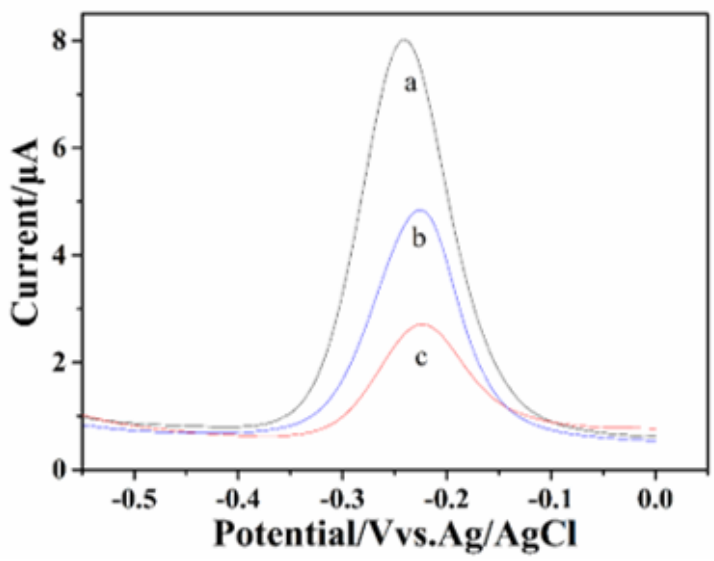

Figure 3

The DPV results of MB on the Exo-I/Apt/cDNA/AuE (a), FB1/Apt/cDNA/AuE (b) and Exo-I/FB1/Apt/cDNA/AuE (c) in Tris-HCl buffer.

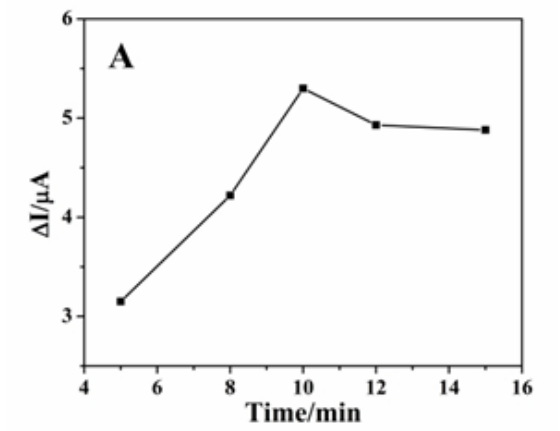

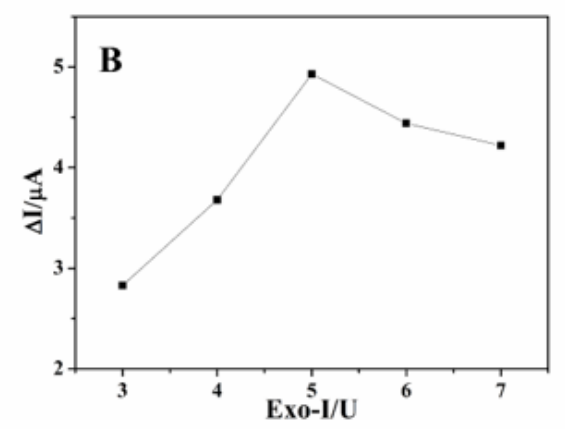

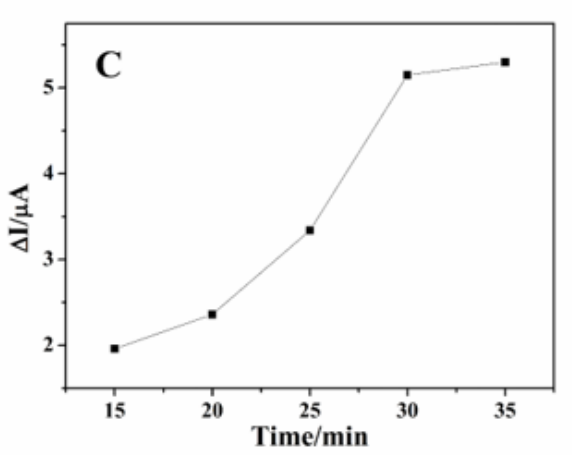

Figure 4

The effect of FB1 incubation time (A), Exo-I amount (B) and Exo-I incubation time (C) on the electrochemical signal.

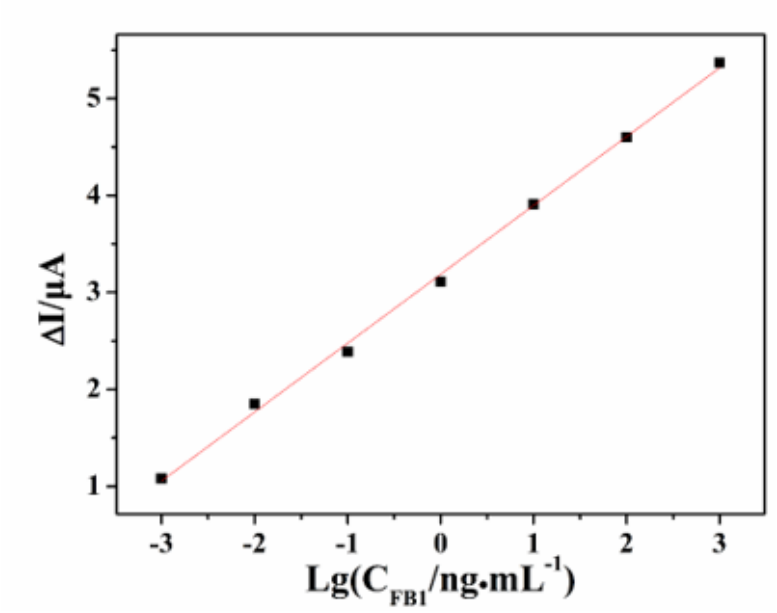

Figure 5

The linear relationship between ΔI and Lg[CFB1] with FB1 concentration in the range of 1×10-3~1000 ng·mL-1.

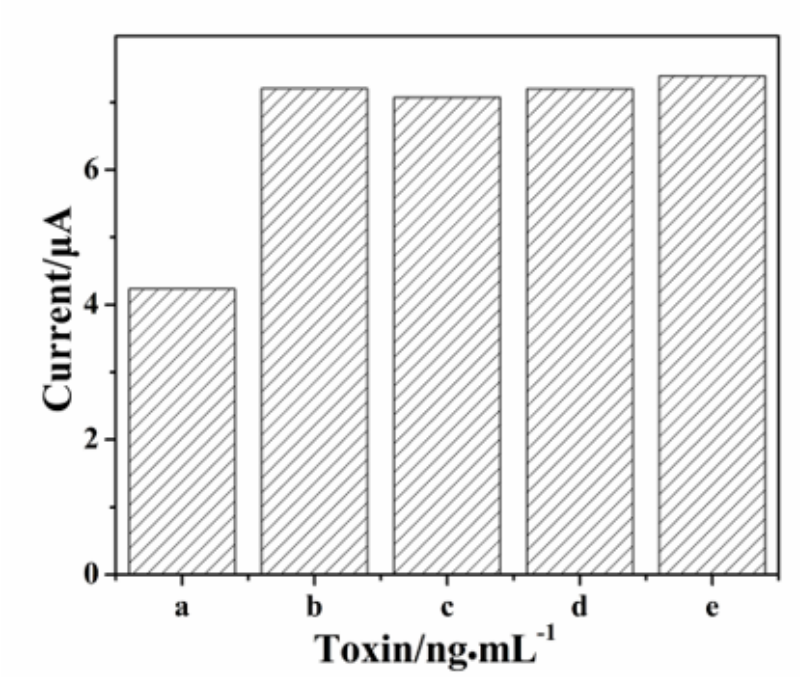

Figure 6

The peak current of aptasensor incubated in different toxins with the same concentration of 1 ng·mL−1. (a) FB1 (b) OTA (c) ZEA (d) AFB1 (e) Blank.